Uric acid activates NRLP3 inflammasome in an in-vivo model of epithelial to mesenchymal transition in the kidney

César Andrés Romero, Aline Remor, Alexandra Latini, Ana Lucía De Paul, Alicia Inés Torres & Jorge Humberto Mukdsi

Journal of Molecular Histology

ISSN 1567-2379
Volume 48
Number 3

J Mol Hist (2017) 48:209-218
DOI 10.1007/s10735-017-9720-9

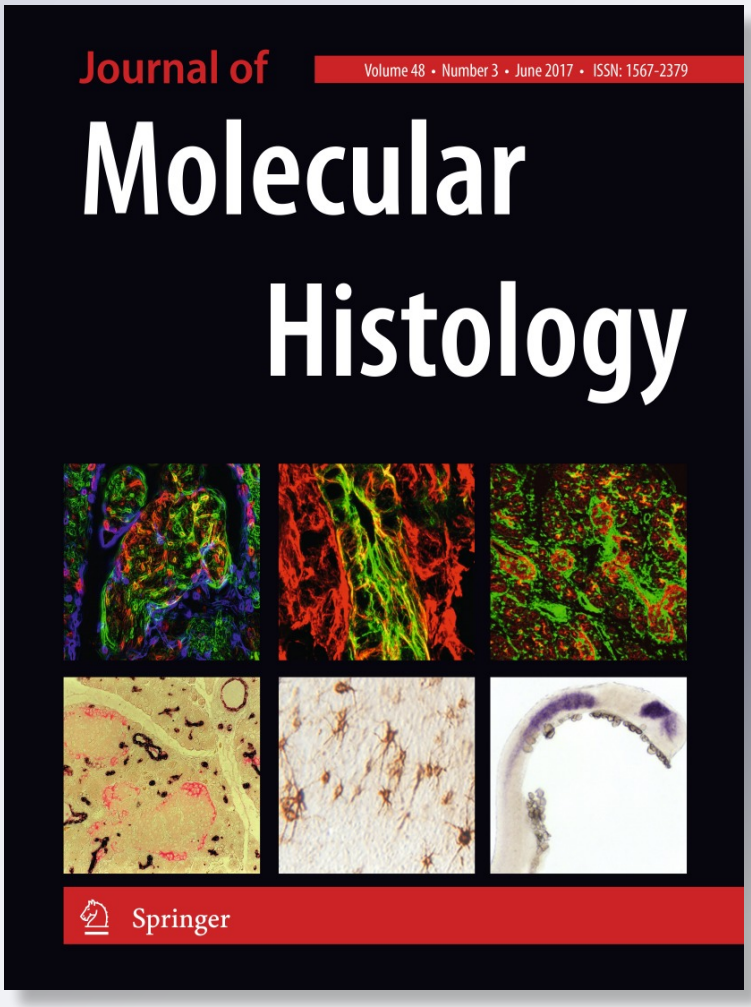

Springer

J Mol Hist (2017) 48:209–218
DOI 10.1007/s10735-017-9720-9

ORIGINAL PAPER

Uric acid activates NRLP3 inflammasome in an in-vivo model of epithelial to mesenchymal transition in the kidney

César Andrés Romero[1] · Aline Remor[2] · Alexandra Latini[2] · Ana Lucía De Paul[1] · Alicia Inés Torres[1] · Jorge Humberto Mukdsi[1]

Received: 9 January 2017 / Accepted: 20 March 2017 / Published online: 3 April 2017

Abstract Uric acid (UA) has been associated with renal fibrosis and progression of chronic kidney disease. However, the underlying mechanisms of this process have still not been identified. Here, we studied the role of the innate imunity receptor NLRP3/ASC in UA induced epithelial-mesenchymal transition (EMT) in kidney. Wistar rats were fed with oxonic acid 2% and UA 2% (OXA + U), OXA + U plus allopurinol (ALL) or regular chow (C) for 7 weeks. We analyzed the presence of EMT markers, the expression of NLRP3, ASC, Caspase-1 and Smad 2/3 molecules and the mitochondrial morphological and functional characteristics. High UA induced renal fibrosis, mild chronic inflammation, as well as morphological and biochemical evidence of EMT. High UA also increased the expression of NLRP3/ASC with activation of both inflammasome related caspase-1 and inflammasome unrelated Smad 2/3 pathways. Ultrastructural co-localization of NLRP3 and Smad 2/3 indicated physical interaction between the two molecules. No morphological or functional changes were found between mitochondria exposed to high UA. In conclusion, kidney epithelial NLRP3/ASC expression was increased in high UA state in rats and both inflammasome related caspase-1 and non-inflammasome related P-Smad 2/3 pathways were associated with the observed EMT, inflammation and fibrosis induced by UA in the kidney.

Keywords Epithelial-mesenchymal transition · Mitochondria · NLRP3/ASC · Smad 2/3 · Uric acid · Kidney

Introduction

Chronic kidney disease (CKD) affects more than 10% of the population (Mills et al. 2015) and is associated with high morbidity, mortality and increased health care costs. Tubular-interstitial fibrosis is a CKD feature, and it has been proposed that some of the fibroblast in CKD may originated from the transformed tubular epithelial cells via epithelial-mesenchymal transition (type II EMT) (Kalluri and Weinberg 2009). Different criteria have been used in identifying epithelial cells undergoing transformation into fibroblast cells in in vivo models, with one of the most important criteria being the expression of fibroblast-specific protein 1 (FSP1) (Strutz et al. 1995; Zeisberg and Neilson 2009). Previous studies have shown hyperuricemia as a risk factor for CKD in the general population (Li et al. 2014) and as a factor that accelerates CDK progression (Rodenbach et al. 2015; Moriyama et al. 2015). In rats, mild hyperuricemia induces tubular-interstitial fibrosis independent of intrarenal crystal formation, and EMT in renal tubular cells (Sanchez-Lozada et al. 2005; Ryu et al. 2013). Recent studies have also shown that innate immunity plays an important role in kidney interstitial inflammation and fibrosis (Leemans et al. 2014). In this regard,

Electronic supplementary material The online version of this article (doi:10.1007/s10735-017-9720-9) contains supplementary material, which is available to authorized users.

✉ Jorge Humberto Mukdsi
mukdsijorge@gmail.com

[1] Facultad de Ciencias Médicas, Centro de Microscopía Electrónica, Instituto de Investigaciones en Ciencias de la Salud (INICSA-CONICET), Universidad Nacional de Córdoba, Av. Haya de la Torre 1er Piso, Ciudad Universitaria, 5000 Córdoba, Argentina

[2] Departamento de Bioquímica, Centro de Ciências Biológicas, Universidade Federal de Santa Catarina, Campus Universitário, 88040-900 Florianópolis, Santa Catarina, Brazil

the cytoplasmatic NLR Family Pyrin Domain Containing 3 (NLRP3) was shown to participate in inflammatory and fibrotic kidney responses in humans and rodents (Vilaysane et al. 2010; Lorenz et al. 2014; Liu et al. 2015). Recently, a NLRP3 inflammasome independent pathway has been proposed, that involves the the trasnformig growth factor-β (TGF-β) signaling mechanism, a phosphorylation of mothers against decapentaplegic homolog (Smad 2/3) (Wang et al. 2013). Moreover, the decreased of TGF-β/Smad2 and the IL-1β signaling was associated with less EMT markers (Wang et al. 2015) and both pathways are related to NLRP3.

It is known that in vitro and in vivo, uric acid (UA) activates NLRP3/ASC inflammasome in the macrophages (Martinon et al. 2006; Usui et al. 2015; Kim et al. 2015). However, NLRP3/ASC expression in epithelial cells is not very well studied during the EMT phenomenon induced by UA. It has been suggested that UA can induce mitochondrial dysfunction; however the studies on NLRP3 activation by ROS did not provide sufficient evidence for proving this hypothesis (Usui et al. 2015; Zhuang et al. 2015; Granata et al. 2015). Allopurinol is an inhibitor of xanthine oxidase enzyme and is the most often used drug to decreased UA in humans. It has also been proposed to decrease the purine synthesis and to have some antioxidant effects (George and Struthers 2009).

In the present study we hypothesized that high UA increases epithelial expression of NLRP3/ASC, and that inflammasome related caspase-1 pathway and non-inflammasome related Smad 2/3 pathway are both associated with EMT and fibrosis in the rat kidneys.

Materials and methods

Animals and experimental design

Male Wistar rats, 200–250 g of body weight (n = 4–6) were used. Animals were kept in accordance with the Guide for the Care and Use of Laboratory Animals (2011). To increase UA concentration in plasma, one group was fed with the food supplemented with 2% oxonic acid (uricase inhibitor) plus 2% UA for 7 weeks (OXA + U). Two control groups were included: *C* group (regular chow without supplements) and *ALL* group (OXA + U plus allopurinol 150 mg/l in drinking water) (Mazzali et al. 2001). At day 0 and at 7 weeks of treatment, plasma UA and urea were measured in the blood samples drawn from tail vein using the commercially availble colorimetric assay kits (Labtest, Brazil). UA (U2625) and oxonic acid (156124) were purchased from Sigma, St. Louis, MO (USA). Allopurinol was purchased from Gador (Argentina).

Renal histology

Renal interstitial area was determined by a point-counting technique using an image analyzer (Image J; NIH, Bethesda, Maryland, USA). Results were expressed as the mean percentage of grid points lying within the interstitial area of up to fifteen consecutive fields in the cortex (Hruska et al. 2000). The tissue fibrosis was evaluated by Masson's trichormic stain and expressed as fractional area. The inflammatory infiltrate was classified as mild (no cells or one foci with less than five cells), moderate (up to two foci with at least five cells) and severe (three or more foci). This analysis was performed by three blinded independent pathologists with a strong agreement shown among the results (Kappa coefficient 0.73; $P < 0.01$). The semiquantitative analysis was performed in images from 15 consecutive fields in the renal cortex of each animal, taken at ×400.

Morphological ultrastructural analyses

Kidney tissue fragments were fixed in 4% glutaraldehyde and 4% formaldehyde in 0.1 M cacodylate buffer, treated with 1% osmium tetroxide, and embedded in Epon/Araldite. Thin sections were examined in a Zeiss LEO 906-E electron microscope and photographed (Megaview III camera). The long axis and the mitochondrial shape of epithelial cells were compared between the groups using images taken with 30,000× magnification (He et al. 2014).

Immunohistochemical analysis and morphometry

Kidney tissue sections were subjected to microwave antigen retrieval in the presence of 0.01 M citrate buffer, pH 6.0 and non-specific binding sites were blocked with 1% goat serum. Tissue sections were then incubated with anti-FSP1 (2 µg/µl, Abcam, Cambridge, UK), anti-vimentin (1:150, Sigma-Aldrich, USA), anti-NLRP3 (1:150, Santa Cruz Biotechnology; Santa Cruz, USA), anti-caspase 1 (1:100 Abcam, Cambridge, UK), anti-ASC (1:100, Sigma-Aldrich, USA) or anti-P-Smad 2/3 (1:100, Millipore, Darmstadt, Germany) primary antibodies. Species-specific secondary antibodies labeled with horseradish peroxidase (HRP) were used. The tubules were counted, and the presence of immune reactive cells in each tubule determined (number of immune reactive cells/tube or percentage of immuno reactive tubules per field).

Ultrastructural immunolabelling

Glutaraldehyde fixed kidney samples were dehydrated using a series of ethanol, and embedded in LR White (London Resin, UK). Anti-FSP1 (diluted 1:50), anti-NLRP3 (diluted 1:50), anti-ASC (diluted 1:50) and anti-P-Smad

2/3 (diluted 1:50) were used as primary antibodies. To detect FSP1, NLRP3, ASC and P-Smad 2/3 positive structures, protein A/colloidal gold complex diluted 1:20 was employed. For co-immulocalization, 15 and 25 nm colloidal gold complexes were used at 1:20 and 1:10 dilutions, respectively.

Functional mitochondrial studies

Respiratory chain enzyme activities

Kidney mitochondria from the OXA + U and C groups were purified for the respiratory chain enzyme activity measurement on complexes I, I–III (Schapira et al. 1990), II, II–III (Fischer et al. 1985), IV–V (Rustin et al. 1994). Briefly, kidney tissue was homogenized and centrifuged at 3000*g* for 10 min at 4 °C, after which the pellets were discarded. To isolate the mitochondria the supernatants were further centrifuged at 17,000*g* for 10 min at 4 °C. Respiratory chain complexes activity was analyzed by spectrophotometry and expressed as nmol/min/mg protein or mmol/min/mg protein.

Respiratory parameters

The rate of oxygen consumption was measured polarographically using a Clark-type electrode in a thermostatically controlled (37 °C) and magnetically stirred incubation chamber of 1.6 ml capacity using Oroborus Oxigraph-2K (Cassina and Radi 1996). The rate of oxygen consumption in these conditions corresponded to state IV, with state III being initiated by adding 250 nmol ADP, and the respiratory control ratio (RCR: state III/state IV) being used as an index of the mitochondrial function (Brand and Nicholls 2011). Similarly, cortical kidney fragments from normal rats were permeabilized for 40 min in saponin at the concentration of 100 µg/ml and then to evaluate the respiratory parameters in whole tissue samples were incubated in the vehicle buffer, or buffer plus 5, 7 and 10 mg/dl of UA. Finally, to analyze the chronic effects of UA on the respiratory parameters, renal mitochondrias from the C and OXA + U groups were isolated and RCR was calculated.

Statistical analysis

Quantitative and qualitative data were expressed as mean ± SD and as a percentage, respectively. *t* test and ANOVA were used for comparison of quantitative variables with a normal distribution, and the Chi square test was utilized for qualitative variables. $P < 0.05$ was considered statistically significant. SPSS (Chicago, Inc, USA) V.17 software was used for these analyses.

Results

Biochemical and functional parameters

After 7 weeks of treatment plasma UA concentration was higher in OXA + U group of rats (2.2 ± 0.5 mg/dl) than in the C and ALL groups of rats (0.9 ± 0.7 mg/dl; 1.0 ± 0.3 mg/dl, respectively) (OXA + U vs. C and ALL, $P < 0.02$; C vs. ALL, $P = 1.0$). Similarly, in OXA + U group of rats urea values were higher (58.8 ± 6 mg/dl) than in C (42 ± 3 mg/dl) and ALL (28.5 ± 2 mg/dl) group of rats (OXA + U vs. C and ALL, $P < 0.001$; C vs. ALL, $P < 0.001$).

Uric acid induces interstitial renal fibrosis and EMT morphological changes

Depressed macroscopic scars on the cortical surface were evident in OXA + U group of rats. Light microscopy analysis revealed that hyperuricemic animals exhibited a significant increase in extracellular matrix as evaluated by Masson´s trichrome technique (13.8% fractional area), compared to the C group of animals (8% fractional area) ($P < 0.001$). Chronic mononuclear inflammatory infiltrate was also observed in the OXA + U group (electronic supplementary material). Ultrastructural analysis demonstrated subcellular morphological changes in the epithelium of the proximal convoluted tubules in the OXA + U group of animals, showing basal membrane disruption and concomitant cytoplasmic epithelial extensions invading the interstitial space (Fig. 1f). These changes were not present in the C group of animals.

Hyperuricemia induces FSP1 expression in epithelial cells

FSP1 immunoreactivity was predominantly found in the vascular walls and the interstitials cells in the C group of rats. The increased UA induced the expression of FSP1 in the epithelial cells (Fig. 1a, b). FSP1 positive cells were increased fivefold in OXA + U animals, compared to the C group of rats ($P < 0.01$) (Fig. 1c). Ultrastructural immunolabeling confirmed the presence of FSP1 within the cytosolic matrices of tubular epithelial cells in the OXA + U group of rats (Fig. 1e, f). The expression analysis of vimentin, another EMT marker, showed a very similar patern to that of the FSP1 protein (Fig. 1g–i).

Overexpression of NLRP3/ASC was induced by uric acid in renal parenchyma

As shown in Fig. 2, in the C group of animals, 5% of the renal tubules were found positive for NLRP3 and ASC,

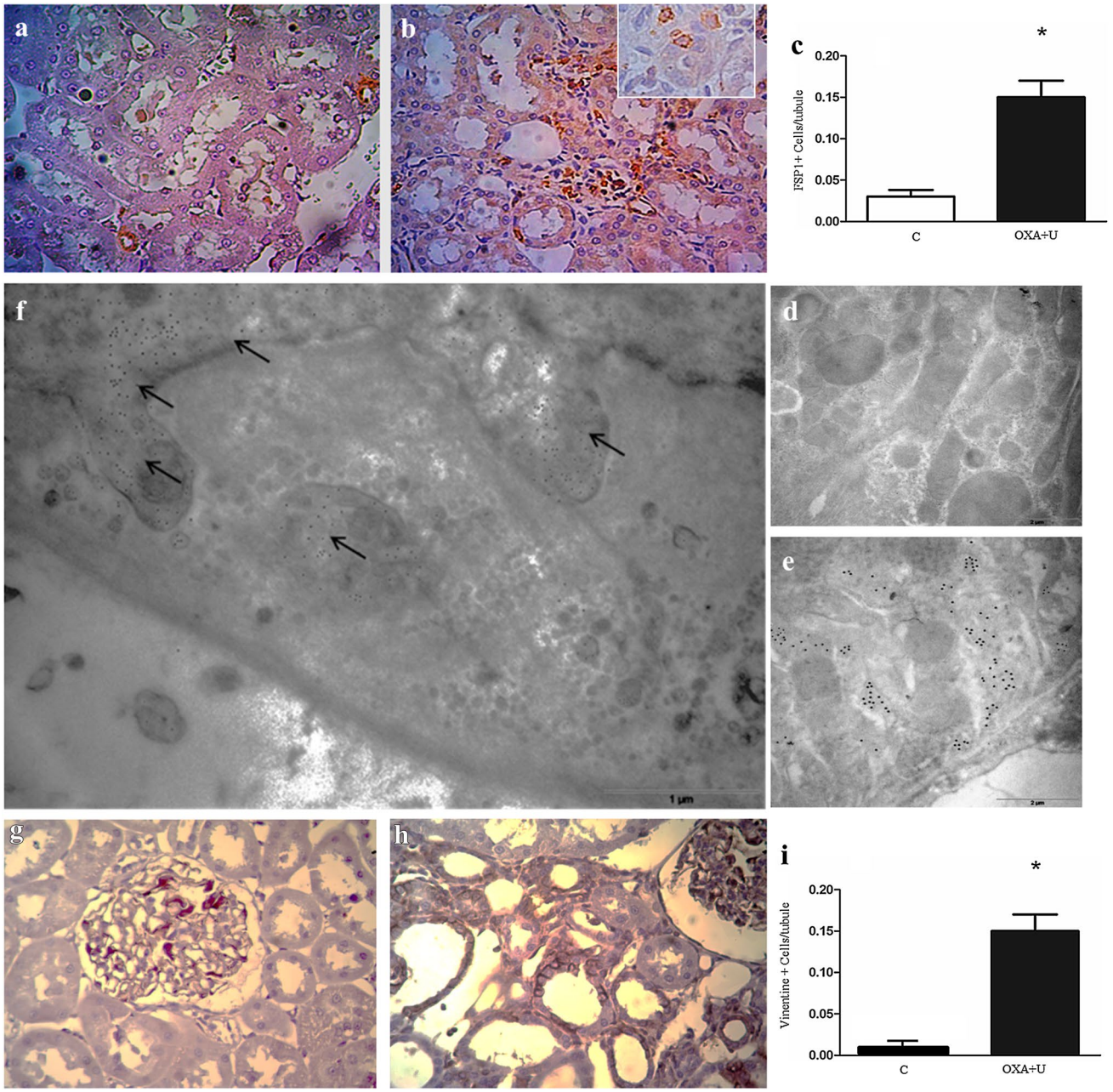

Fig. 1 Fibroblastic specific protein type 1 (FSP1) inmunolabelling. Normouricemic animals show FSP1 expression, mostly in vascular walls and some interstitial fibroblast (**a**). No immunostaining was observed in tubular epithelial cells by light microscopy (**a**) or electron microscopy (**d**). Hyperuricemic animals show a significant increase of FSP1 protein expression in interstitial cells and renal epithelial cells (**b, c, e**). **b***Inset* shows a 400× magnification of a positive FSP1 immunoreactivity in tubular epithelial cell immune-reactive. (**f**) Electron microscopy micrograph showing basal portion of tubular epithelial cell undrgoing EMT process, cytoplasmatic extension invading a tubular basement membrane and immunostaining for FSP1 (*arrow*). **a, b** Original magnification 200×. (*$P<0.001$ vs. C). Vimentin immunostaining. Normouricemic animals (**g, i**) show vimentin expression only at glomerular level, whereas OXA + U treatment induced a significant increase of this protein in renal epithelial cells (**h, i**). **a, b, g, h** Original magnification 200×. (*$P<0.001$ vs. C)

whereas in the OXA + U group of rats NLRP3 immunoreactivity was detected in 67% of the analysed tubules ($P<0.01$). Allopurinol treatment prevented these changes. Moreover, in hyperuricemic animal ultrastructural analysis of the immunoreactivity confirmed NLRP3 and ASC protein expression in the epithelial tubular cells within the cytosolic and mitochondrial matrices (Fig. 3a, b). Interestingly, NLRP3 and ASC were colocalized in the tubular epithelium, as shown in Fig. 3c, indicating an inflammosome activation.

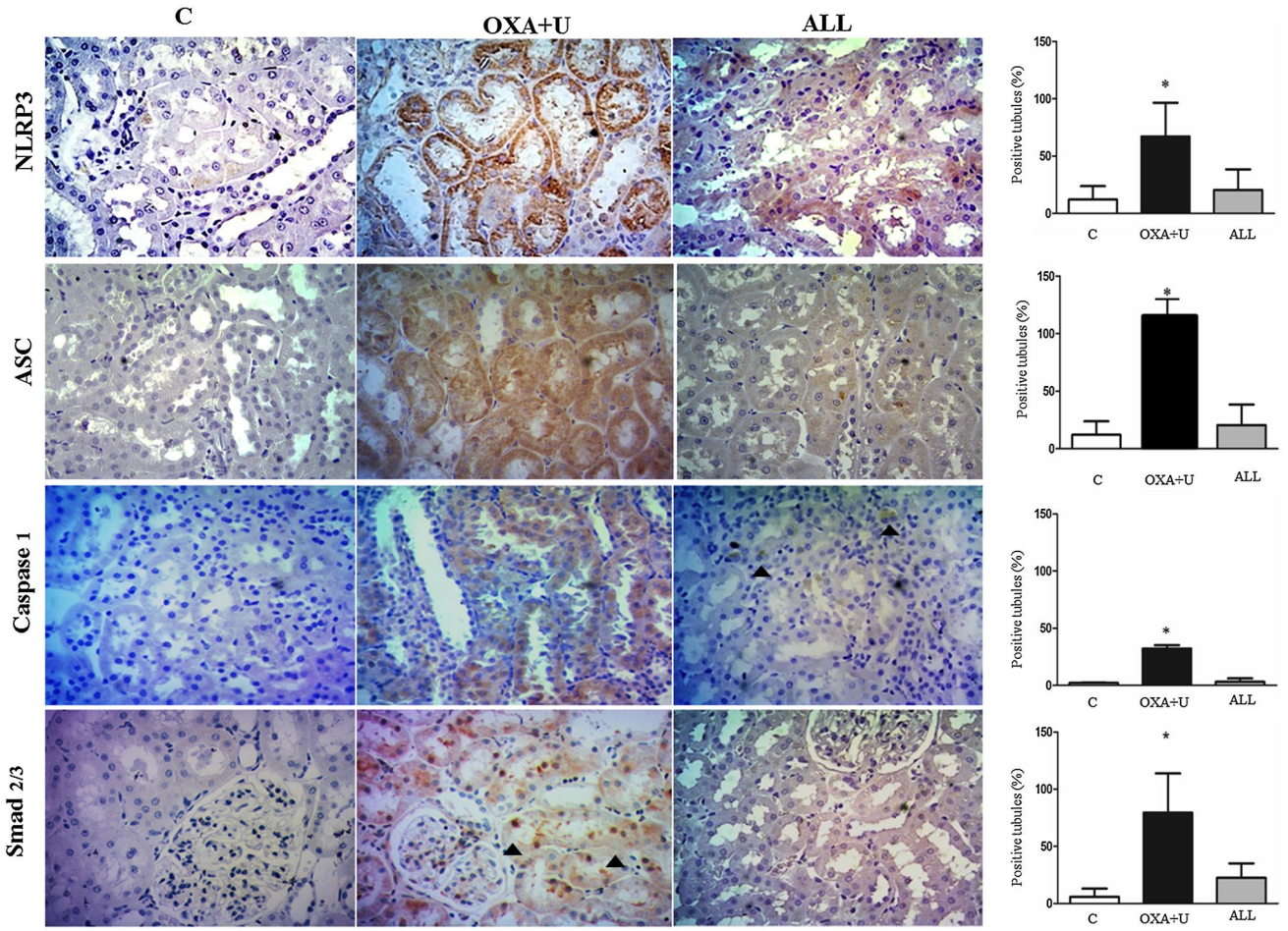

Fig. 2 Immunostaining for NLRP3, ASC, Caspase-1 (inflammasome related) and p-Smad2/3 (inflammasome non-related) pathways in control (C), high uric acid (OXA + U) and allopurinol (ALL) treated groups. High uric acid significantly increased NLRP3, Caspase-1 and Smad 2/3 expression compared with C group of animals, and allopurinol treated group decrease the expression of NLRP3 receptor and the inflammasome related and non-related pathways. Original magnification 400×. (*$P < 0.001$ vs. C and ALL)

Hyperuricemia increased the expression of both inflammasome related caspase-1 and non inflammasome related Smad 2/3 pathways in kidney

Caspase-1 was expressed in 2% of the analysed tubule in the C group of animals, while 32% of the tubules from the OXA + U group of animals showed immunereactivity to Caspase-1 in the tubular epithelial cells that was suppressed by allopurinol (Fig. 3). Phosphorylated Smad 2/3 protein was also increased in the OXA + U group of animals compared to the C and ALL groups, with the tubular epithelial cells exhibiting immunoreactivity at both the cytoplasmic and the nuclear levels (Figs. 2, 3d). Quantitative analysis showed a significant reduction of P-Smad 2/3 in the ALL group of animals (OXA + U 79.4 ± 34.4%; C group 5.8 ± 0.3%; ALL 22.4 ± 12.6%; $P < 0.01$).

Uric acid associates with NLRP3 and Smad 2/3 colocalization

High UA induced a colocalization of NLRP3 and P-Smad 2/3 molecules in the cytosolic matrix. Specific pattern of several P-Smad 2/3 molecules around the NLRP3 molecule was observed. The distance between colloidal gold particles varied from 16 to 60 nm, indicating a possible physical interaction (Fig. 3f). Both molecules were present in the C group of animals, but no interaction was observed (Fig. 3e). In the C group of animals NLRP3 was not detected in the mitochondrial compartment, and P-Smad 2/3 did not translocate to the nucleus.

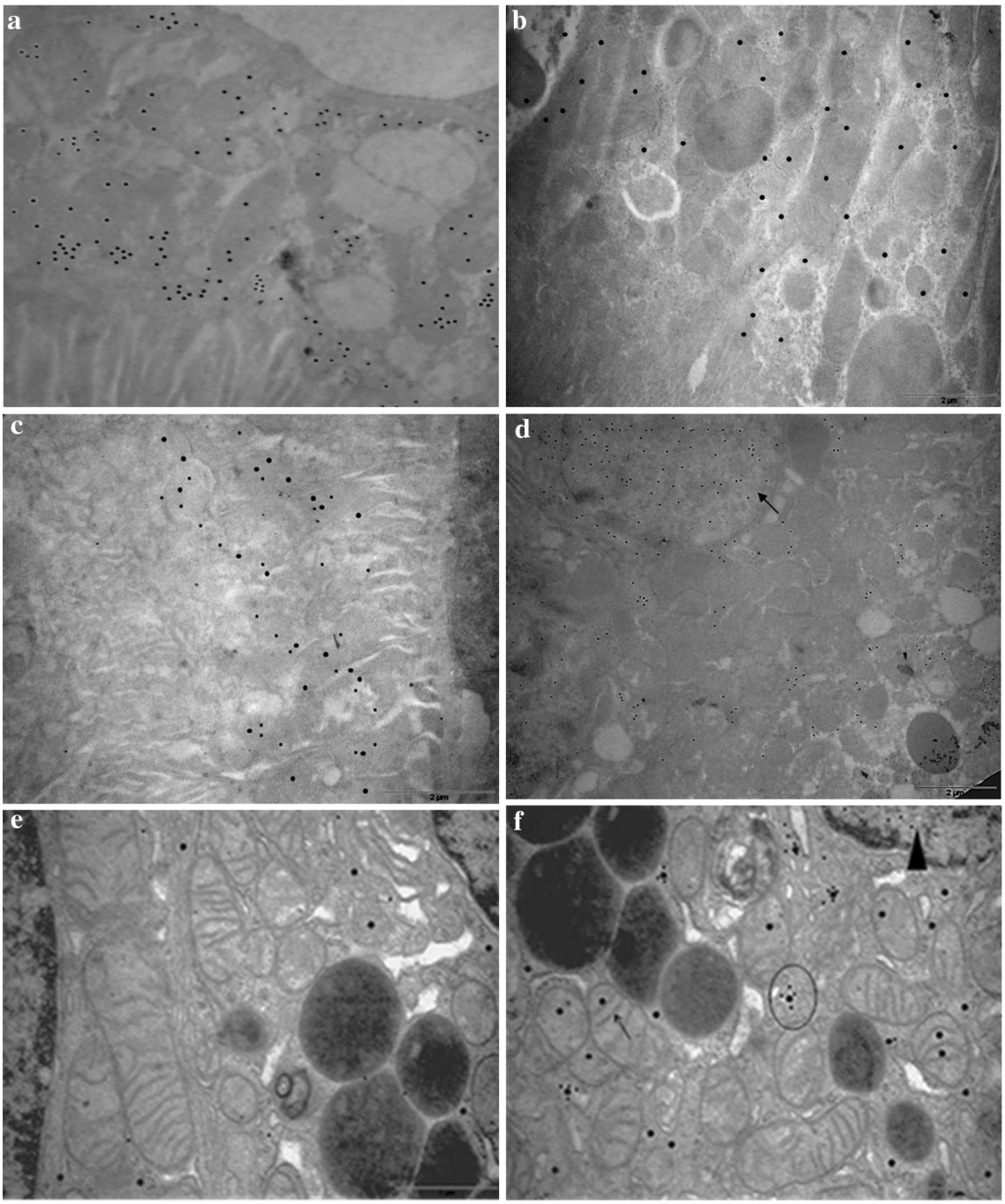

Fig. 3 Ultrastructural expression of NLRP3, ASC and P-Smad 2/3. In hyperuricemic rats NLRP3 receptor (**a**) and ASC (**b**) were detected in cytoplasm of epithelial cells in the proximal tubule, in both cytosolic matrix and mitrochondrial structures. Doble immunostainig for NLRP3 (small gold particle) and ASC (big gold particle) demonstrated inflammosome activation (**c**). **d** Shows P-Smad 2/3 present in cytosolic matrix and in the nucleus (*arrow*) in high UA group of rats. The ultrastructural co-immunolocalization of NLRP3 (big gold particle) and P-Smad 2/3 (small gold particle) indicates a possible interaction between the two molecules in cytosolic matrix of high UA group of rats (**f**, *circle*), whereas in the control groups (**e**) this colocalization was not observed

Effects of uric acid in renal mitochondria

The ultrastructural analysis of 180 mitochondrias from the AOX + U and C groups of animals did not reveal any differences (Fig. 3e, f). Thus, the long axis and the shape index were similar between the groups (Fig. 4a, b).

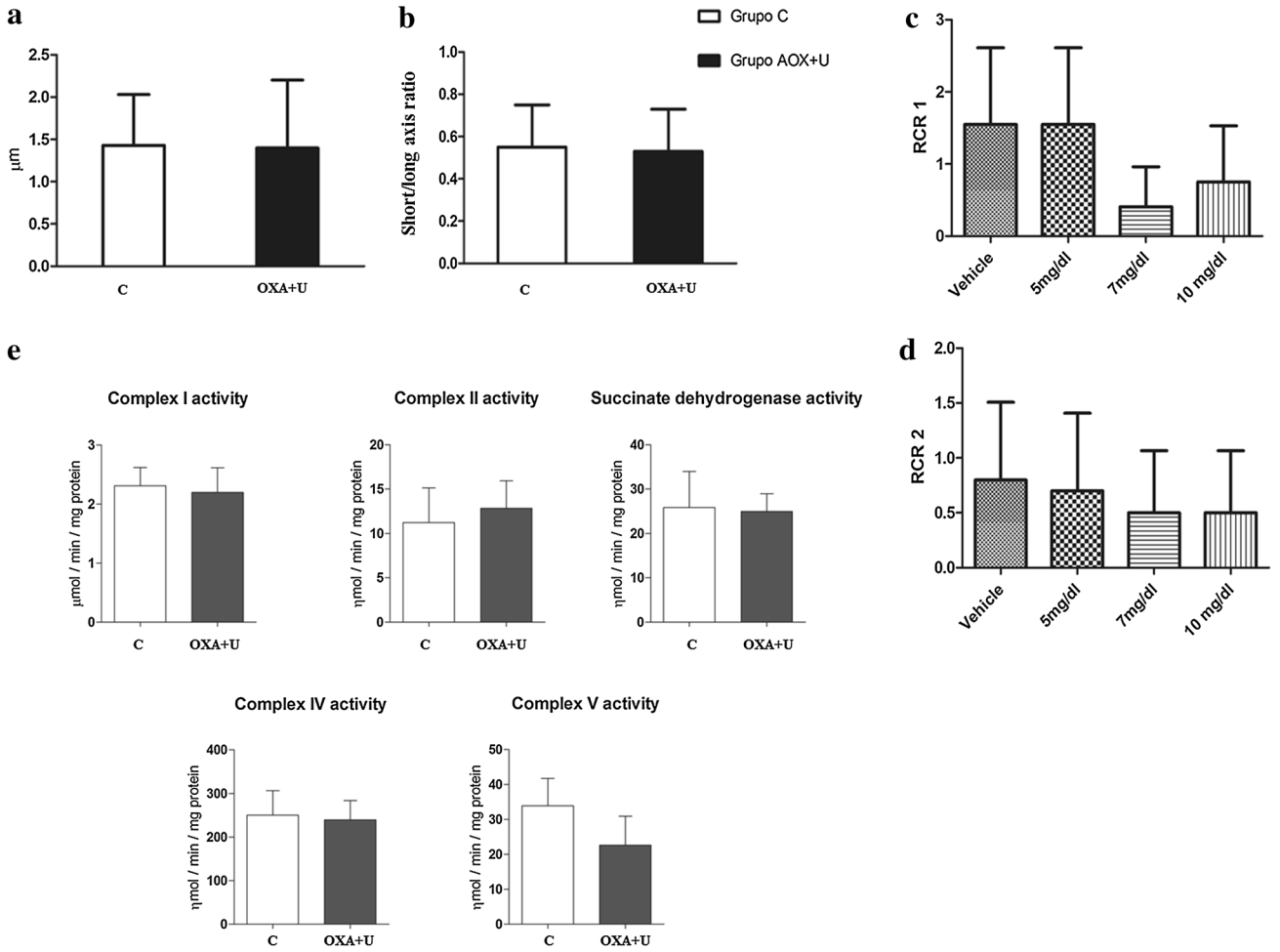

Fig. 4 Morphological and functional analysis of epithelial mitochindrias. **a, b** Shows no differences between the control (C) and high uric acid group (OXA + U) of animals, in length or short/long axis ratio. The in vitro exposition to increasing levels of uric acid reveals a tendency to reduce the respiratory control ratio (**c, d**). However, this was not statistically significant ($P = 0.2$). Chronic exposition of high uric acid did not alter the enzymatic activity of the mitochondrial complex (**e**)

Respiratory parameters

In-vitro acute mitochondria exposition to the increasing levels of UA did not show any differences in RCR associated to NAD-linked and FAD-linked substrates (Fig. 4c, d) or in whole kidney tissue samples from normal Wistar rats. Chronic exposition to high UA did not reveal any differences in ex-vivo enzymatic activity of the mitocondrial respiratory complexes I–V between the OXA + U and C group of animal (Fig. 4e).

Discussion

Epidemiological studies have shown the association between plasma UA concentration and renal damage. In this study, using rat animal model we demonstrated UA induced inflammation, EMT and fibrosis as well as the innate immunity role in these processes throught the NLRP3/ASC receptor and pathways.

Despite that the EMT have been demonstrated in vivo by Strutz et al. (1995), this phenomenom is still disputed by some investigators due to the lack of in vivo evidence showing cells with fibroblast characteristics within the tubular basement membrane (TBM) or a crossing the TBM (Kriz et al. 2011). Here, we have demonstarted EMT major and minor criterias, as well as epithelial tubular cells expressing the specific mesenchymal FSP1 marker crossing through a disrupted TBM. In addition these cells exhibited overexpression of vimentin. Therefore we confirmed the in vivo existence of EMT and the pathogenic role of UA in kidney fibrosis (Ryu et al. 2013). We also demonstrated the presence of a low grade tubulo-intersticial inflammation and fibrosis that was in agreement with previous reports

(Mazzali et al. 2001; Kim et al. 2015). Although UA nephropathy can induce aseptic inflammation, similarly to the previous reports (Mazzali et al. 2001), we did not find any direct or indirect sign of crystal deposition in the kidney parenchyma by light or electron microscopy.

The underlying mechanism through which UA may induce inflammation and EMT is unclear. However, some reports have proposed an activation of RAAS, NOS and TGF-β signaling (Khosla et al. 2005; Talaat and el-Sheikh 2007). It has been postulated that NLRP3/ASC associated with caspase-1 can induce the mature form of IL-1β and IL-18 and consequently a local inflammation and that through the non-canonical pathway, NLRP3/ASC can interact with TGF-β signaling, thereby increasing the phosphorylated Smad 2/3 molecule, which can then induce the EMT program through Smad-R (Wang et al. 2013; Lorenz et al. 2014). Moreover, the decreased of TGF-β/Smad2 and the IL-1β signaling was associated with less EMT markers in obstructive kidney diseases (Wang et al. 2015) and both pathways are related to NLRP3. Considering that UA can activate the NLRP3/ASC, we hypothesized that mechanisms of UA induced kidney changes may involve NLRP3/ASC receptor (Martinon et al. 2006). We observed a dramatic increase in the expression of NLRP3/ASC in tubular epithelial cells in animals exposed to the high concentrations of UA for 7 weeks. Allopurinol treatment prevented the augmented NLRP3/ASC expression. In normal control group of rats, only 5% of the renal tubules were positive for these proteins. Previous report has demonstrated lower NLRP3 mRNA levels in normal kidneys in comparison to the mRNA levels of the other NLR type molecules (Lech et al. 2010). Interestingly, in OXA + U group of animals in addition to cytosolic matrix localization, we found NLRP3/ASC expression at the mitochondrial level. Although mitochondrial abnormalities were not present, this NLRP3/ASC localization indicates that this organelle may act as a platform to recruit additional members of the inflammasome (Zhou et al. 2011). Other study showed that NLRP3/ASC activation induced its redistribution by migrating from cytoplasmic regions into the mitochondria and smooth endoplasmic reticulum (Zhou et al. 2011). On the other hand, Granata et al. have demonstrated colocalization of NLRP3/ASC/mitochondria in peripheral blood mononuclear cells from CKD-Hemodialysis patients, concluding that this condition could possibly be induced by mitochondrial dysfunction (2015).

Similarly to the increase in NLRP3 expression, we found an increased expression of caspase-1 and P-Smad 2/3 in kidney tubular ephitelial cells. At the ultrastructural level, most of the P-Smad 2/3 molecules translocated into the nucleus. A critical role of NLRP3 on Smad 2/3 phosphorilation was reported to happen after the TGF-β stimulus. However, it was not clear if there was a direct or indirect interaction between the molecules, since the previus attempt to co-inmmunoprecipitate NLRP3 and Smad 2/3 failed (Wang et al. 2013). In this context, we performed an ultrastructural co-inmunolocalization analysis of NLRP3 and P-Smad 2/3. In addition to the distribution described for NLRP3 and Smad 2/3, we detected a perinuclear characteristic pattern of distribution containg of several P-Smad 2/3 surrounding the NLRP3 molecule. This pattern was not present in the C group of animals or in the negatives controls, discounting any steric effect. This suggests a physical interaction between the two molecules, and supports the previous reports where activated NLRP3 was shown to bound to mitochondria migrated to the perinuclear area (Zhou et al. 2011). The functional aspect of this phenomenon is still not understood, but it may play a role in the Smad 2/3 phosphorylation before its nuclear translocation.

Several mechanisms can activate the NLRP3/ASC receptor, with mitochondrial dysfunction and subsequent ROS production, lysosomal destabilization and potassium efflux being the most important (Sutterwala et al. 2014). Considering previous reports on mitochondrial dysfunction induced by UA and the observed interaction between mitochondrias and NLRP3 protein (Zhuang et al. 2015), we studied the morphological and physiological mitochondrial changes induced by UA in in vitro and in vivo experiments. Unexpectedly, no differences were found in either of morphological or physiological mitochondrial characteristics. Similarly, our in vitro research determinated that at the physiological levels, UA was unable to produce any abnormalities in the isolated mitochondria. It has been suggested that UA can induce a mitochondrial dysfunction (Sanchez-Lozada et al. 2012), however, in these reports the UA levels were higher than 10 mg/dl, and the mitochondrial function was measured through indirect markers. Other report has shown mitochondrial alterations when exposed to UA, but this modification only appeared after 12 weeks of treatment and was not present at 7 weeks, when all the inflammatory and fibrotic characteristics were detected (Cristobal-Garcia et al. 2015). This indicates that mitochondrial abnormalities reported in that work may be rather a consequence of a chronic inflammation than a direct UA effect. Nevertheless, Usui et al. (2015) showed that the effect of activation of NLRP3 by angiotensin II on macrophages was mediated by mitochondrial dysfunction, whereas mitochondrial alterations were not present when macrophages were activated by UA. Thus, future studies are necessary to better understand the molecular activation of NLRP3 by UA in in vivo.

Finally, to explore the interaction between NLRP3 and Smad 2/3, we performed an ultrastructural co-inmunolocalization. Although, this technique has produced reliable results in previous investigation (Petiti et al. 2015), we are aware of the limitations of this methodology in demonstarting the physical interaction. Nevertheless, considering that

previous report (Wang et al. 2013) showed strong evidence supporting this interaction and that to date their colocalization has not been shown, our data significantly contributes to the present knowledge in this field. We conclude that the NLRP3/ASC receptor expression was increased in tubular epithelial cells in a high UA state in rats, and that inflammasome related caspase-1 and non-inflammasome related P-Smad 2/3 pathways both associated with UA induced EMT, inflammation and fibrosis in kidney.

Our data will help understand parts of the mechanisms mediated by UA in the progression of CKD and consenquently aid the development of new therapies preventing the CKD progression.

Acknowledgements The authors thanks to Dr. Carolina Leimgruber, Mrs. Lucia Artino, Mrs. Maria Elena Pereyra, and Miss. María Soledad Santa Cruz for their technical support. We would also like to thank native speaker Dr. Paul Hobson for editing the English language of the manuscript.

Funding This work was funded by the grants from Secretaria de Ciencia y Tecnologia from National University of Cordoba (Secyt, UNC) and Fondo para la Investigacion Cientifica y Tecnología (FonCyT), de la Agencia Nacional Cientifica y Tecnología.

Compliance with ethical standards

Conflict of interest All the authors declare that they have conflict of interest related to this work and approved the final version of the manuscript.

References

Brand MD, Nicholls DG (2011) Assessing mitochondrial dysfunction in cells. Biochem J 435:297–312. doi:10.1042/BJ20110162

Cassina A, Radi R (1996) Differential inhibitory action of nitric oxide and peroxynitrite on mitochondrial electron transport. Arch Biochem Biophys 328:309–316. doi:10.1006/abbi.1996.0178

Cristobal-Garcia M, Garcia-Arroyo FE, Tapia E et al (2015) Renal oxidative stress induced by long-term hyperuricemia alters mitochondrial function and maintains systemic hypertension. Oxid Med Cell Longev 2015:535686. doi:10.1155/2015/535686

Fischer JC, Ruitenbeek W, Berden JA et al (1985) Differential investigation of the capacity of succinate oxidation in human skeletal muscle. Clin Chim Acta 153:23–36

George J, Struthers AD (2009) Role of urate, xanthine oxidase and the effects of allopurinol in vascular oxidative stress. Vasc Health Risk Manag 5:265–272. doi:10.2147/VHRM.S4265

Granata S, Masola V, Zoratti E et al (2015) NLRP3 inflammasome activation in dialyzed chronic kidney disease patients. PLoS One 10:1–16. doi:10.1371/journal.pone.0122272

He X, Liu Y, Usa K, et al (2014) Ultrastructure of mitochondria and the endoplasmic reticulum in renal tubules of Dahl salt-sensitive rats. Am J Physiol Renal Physiol 306:F1190–F1197. doi:10.1152/ajprenal.00073.2014

Hruska KA, Guo G, Wozniak M et al (2000) Osteogenic protein-1 prevents renal fibrogenesis associated with ureteral obstruction. Am J Physiol Renal Physiol 279:F130–F143

Kalluri R, Weinberg RA (2009) The basics of epithelial-mesenchymal transition. J Clin Invest 119:1420–1428. doi:10.1172/JCI39104

Khosla UM, Zharikov S, Finch JL et al (2005) Hyperuricemia induces endothelial dysfunction. Kidney Int 67:1739–1742. doi:10.1111/j.1523-1755.2005.00273.x

Kim SM, Lee SH, Kim YG et al (2015) Hyperuricemia-induced NLRP3 activation of macrophages contributes to the progression of diabetic nephropathy. Am J Physiol Renal Physiol 308:F993–F1003. doi:10.1152/ajprenal.00637.2014

Kriz W, Kaissling B, Le Hir M (2011) Epithelial-mesenchymal transition (EMT) in kidney fibrosis: fact or fantasy? J Clin Invest 121:468–474. doi:10.1172/JCI44595

Lech M, Avila-Ferrufino A, Skuginna V et al (2010) Quantitative expression of RIG-like helicase, NOD-like receptor and inflammasome-related mRNAs in humans and mice. Int Immunol 22:717–728. doi:10.1093/intimm/dxq058

Leemans JC, Kors L, Anders HJ et al (2014) Pattern recognition receptors and the inflammasome in kidney disease. Nat Rev Nephrol 10:398–414. doi:10.1038/nrneph.2014.91

Li L, Yang C, Zhao Y et al (2014) Is hyperuricemia an independent risk factor for new-onset chronic kidney disease? A systematic review and meta-analysis based on observational cohort studies. BMC Nephrol 15:122. doi:10.1186/1471-2369-15-122

Liu D, Wen Y, Tang TT et al (2015) Megalin/Cubulin-Lysosome-mediated albumin reabsorption is involved in the tubular cell activation of NLRP3 inflammasome and tubulointerstitial inflammation. J Biol Chem 290:18018–18028. doi:10.1074/jbc.M115.662064

Lorenz G, Darisipudi MN, Anders HJ (2014) Canonical and non-canonical effects of the NLRP3 inflammasome in kidney inflammation and fibrosis. Nephrology, dialysis, transplantation: official publication of the European Dialysis and Transplant Association—European Renal Association. Nephrol Dial Transplant 29:41–48. doi:10.1093/ndt/gft332

Martinon F, Petrilli V, Mayor A et al (2006) Gout-associated uric acid crystals activate the NALP3 inflammasome. Nature 440:237–241. doi:10.1038/nature04516

Mazzali M, Hughes J, Kim YG et al (2001) Elevated uric acid increases blood pressure in the rat by a novel crystal-independent mechanism. Hypertension 38:1101–1106. doi:10.1161/hy1101.092839

Mills KT, Xu Y, Zhang W et al (2015) A systematic analysis of worldwide population-based data on the global burden of chronic kidney disease in 2010. Kidney Int 88:950–957. doi:10.1038/ki.2015.230

Moriyama T, Itabashi M, Takei T et al (2015) High uric acid level is a risk factor for progression of IgA nephropathy with chronic kidney disease stage G3a. J Nephrol 28:451–456. doi:10.1007/s40620-014-0154-0

In: Guide for the care and use of laboratory animals (2011) Committee for the Update of the Guide care and use of laboratory animals. National Academy of Sciences. Chapter 2nd, 3rd, and 8th edn. Washington, DC

Petiti JP, Sosa Ldel V, Sabatino ME et al (2015) Involvement of MEK/ERK1/2 and PI3K/Akt pathways in the refractory behavior of GH3B6 pituitary tumor cells to the inhibitory effect of TGF-beta1. Endocrinology 156:534–547. doi:10.1210/en.2014-1070

Rodenbach KE, Schneider MF, Furth SL et al (2015) Hyperuricemia and progression of CKD in children and adolescents: the chronic kidney disease in children (CKiD) cohort study. Am J Kidney Dis 66:984–992. doi:10.1053/j.ajkd.2015.06.015

Rustin P, Chretien D, Bourgeron T et al (1994) Biochemical and molecular investigations in respiratory chain deficiencies. Clin Chim Acta 228:35–51

Ryu ES, Kim MJ, Shin HS, et al (2013) Uric acid-induced phenotypic transition of renal tubular cells as a novel mechanism of chronic kidney disease. Am J Physiol Renal Physiol 304:F471–F480. doi:10.1152/ajprenal.00560.2012

Sanchez-Lozada LG, Tapia E, Santamaria J et al (2005) Mild hyperuricemia induces vasoconstriction and maintains glomerular hypertension in normal and remnant kidney rats. Kidney Int 67:237–247. doi:10.1111/j.1523-1755.2005.00074.x

Sanchez-Lozada LG, Lanaspa MA, Cristobal-Garcia M et al (2012) Uric acid-induced endothelial dysfunction is associated with mitochondrial alterations and decreased intracellular ATP concentrations. Nephron Exp Nephrol 121:e71–e78. doi:10.1159/000345509

Schapira AH, Cooper JM, Dexter D et al (1990) Mitochondrial complex I deficiency in Parkinson's disease. J Neurochem 54:823–827

Strutz F, Okada H, Lo CW et al (1995) Identification and characterization of a fibroblast marker: FSP1. J Cell Biol 130:393–405

Sutterwala FS, Haasken S, Cassel SL (2014) Mechanism of NLRP3 inflammasome activation. Ann N Y Acad Sci 1319:82–95. doi:10.1111/nyas.12458

Talaat KM, el-Sheikh AR (2007) The effect of mild hyperuricemia on urinary transforming growth factor beta and the progression of chronic kidney disease. Am J Nephrol 27:435–440. doi:10.1159/000105142

Usui F, Shirasuna K, Kimura H et al (2015) Inflammasome activation by mitochondrial oxidative stress in macrophages leads to the development of angiotensin II-induced aortic aneurysm. Arterioscler Thromb Vasc Biol 35:127–136. doi:10.1161/ATVBAHA.114.303763

Vilaysane A, Chun J, Seamone ME et al (2010) The NLRP3 inflammasome promotes renal inflammation and contributes to CKD. Am J Soc Nephrol 21:1732–1744. doi:10.1681/ASN.2010020143

Wang W, Wang X, Chun J et al (2013) Inflammasome-independent NLRP3 augments TGF-beta signaling in kidney epithelium. J Immunol 190:1239–1249. doi:10.4049/jimmunol.1201959

Wang W, Zhou PH, Xu CG et al (2015) Baicalein attenuates renal fibrosis by inhibiting inflammation via down-regulating NF-κB and MAPK signal pathways. J Mol Histol 46:283–290. doi:10.1007/s10735-015-9621-8

Zeisberg M, Neilson EG (2009) Biomarkers for epithelial-mesenchymal transitions. J Clin Invest 119:1429–1437. doi:10.1172/JCI36183

Zhou R, Yazdi AS, Menu P et al (2011) A role for mitochondria in NLRP3 inflammasome activation. Nature 469:221–225. doi:10.1038/nature09663

Zhuang Y, Yasinta M, Hu C et al (2015) Mitochondrial dysfunction confers albumin-induced NLRP3 inflammasome activation and renal tubular injury. Am J Physiol Renal Physiol 308:F857–F866. doi:10.1152/ajprenal.00203.2014